Holmboe modes revisited

O. M. Umurhan[a)]
Department of Physics, Technion—Israel Institute of Technology, 32000 Haifa, Israel
and Department of Astronomy, City College of San Francisco, San Francisco, California 94112

E. Heifetz[b)]
Department of Geophysics and Planetary Sciences, Tel-Aviv University, 69978 Tel-Aviv, Israel

(Received 31 July 2006; accepted 22 February 2007; published online 27 June 2007)

A scaling analysis is presented better identifying the conditions in which the Boussinesq approximation may be used to study shear disturbances like that of Holmboe modes. The classic Holmboe normal mode instability is then reanalyzed by including baroclinic effects whose introduction alters the onset of Holmboe's traveling-wave instability depending on the direction of the propagating modes. Since the introduction of baroclinicity is tantamount to relaxing the Boussinesq assumption, it means that in the presence of shear there is now a vertical variation of the horizontal momentum flux that alters the phase speed and structure of the classic Holmboe modes; the physical source of their broken right-left propagatory symmetry is associated with this physical effect. Furthermore, the regions of parameter space in which Holmboe's classic analysis predicts there to be nonpropagating double instabilities now supports propagating Holmboe modes when baroclinic effects are included. We also find that a globally constant shear profile behaves as a stabilizing agent, in contradiction to the destabilizing role that shear normally plays in the classic Kelvin-Helmholtz problem of a shear-density interface. The general relationship between the normal modes of this type of system to that of the continuous spectrum is also noted. We also find that the baroclinic effects explored here probably do not manifest in terrestrial oceanographic and laboratory conditions, although they may do so in atmospheres. © *2007 American Institute of Physics*. [DOI: 10.1063/1.2730544]

I. INTRODUCTION

A mathematically convenient and conceptually effective way to model an atmospheric flow in which there is both a density gradient and a variation of the horizontal shear is to appeal to the Taylor-Goldstein (TG) equation.[1,2] The model assumptions are essentially that of incompressible flow viewed from the standpoint of the Boussinesq approximation, namely that variations of the density field are dynamically significant only when they couple to the external gravitational field (or, in principle, any externally imposed force upon the system). A rereading of the original treatises of Taylor and Goldstein reveals that the assumptions that go into justifying its use are reasonable provided certain conditions of the dynamics are met. There are mainly two suppositions: (a) the dynamic length scales are short compared to the scale height of the density variation of the atmosphere, and (b) the buoyancy time over the dynamic length scale of the atmosphere is short compared to the typical shear time over the same length scales. In practice, then, variations of the steady density profile (due to stratification) are neglected wholesale except when coupled to gravity, hence the resulting Boussinesq set. Those neglected density fluctuation terms, i.e., those not coupled to the external gravity, are usually termed *the baroclinic effects*.

The use of the TG equation is successful in revealing interesting dynamics that are inherent to such flows. A thorough list is beyond the scope of this introduction, however one of the more interesting results to emerge is the discovery, originally by Holmboe,[3] of dynamical instabilities existing in atmospheres that are otherwise stable to buoyancy oscillations. Holmboe's analysis was to take the problem of a finite shear layer in an unbounded domain, originally solved by Rayleigh,[4] and to place a jump in the density profile midway in the constant shear layer itself. As a reminder, Rayleigh modeled the finiteness of the shear layer by considering the shear to be constant inside the layer and for there to be step-function jumps in the shear profile at the two boundaries of the shear layer (e.g., see Fig. 1). This means, then, that the problem investigated by Holmboe has three stark discontinuities, further implying that these locations of the flow are sources of delta functions of the mean vorticity gradient, leading to either constant vorticity layers in two dimensions or sheets in three dimensions in the disturbances. Holmboe discovered that under certain conditions there are pairs of traveling-wave instabilities supported by such a model configuration. The extent and scope of this particular type of stratified shear instability[5,6] have been observed to some extent in laboratory experiments[7] and explored to further theoretical detail by numerous authors under a variety of conditions, including those that go beyond the conceptually simple situation of a sharp interface.[8–12]

We do not dispute, per se, using delta functions to model variations of shear or density in atmospheres since such tools prove to be useful in both solving problems analytically and

[a)]Electronic mail: mumurhan@physics.technion.ac.il
[b)]Electronic mail: eyalh@cyclone.tau.ac.il

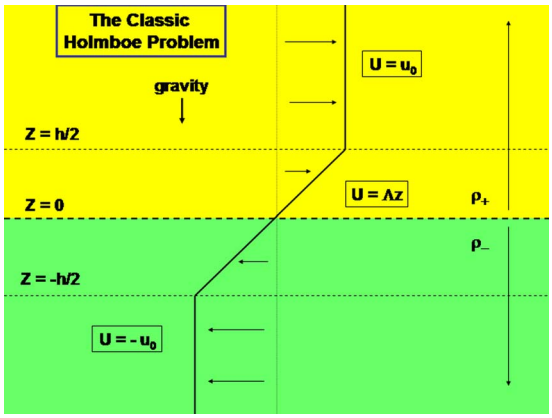

FIG. 1. (Color online) A schematic for Holmboe's problem. This configuration reduces to Rayleigh's problem (Ref. 3) when the two densities are the same.

aiding one in developing a mechanistic understanding of the underlying physics shaping any emergent dynamical activity. For instance, the conceptual tool of Rossby edge waves[13] to interpret the instability of shear layers such as Rayleigh's problem is a fruit borne out by this aforementioned tack. We ask here a different question: under what physical conditions might the Boussinesq approximation (i.e., neglecting the baroclinic effects) not be entirely appropriate? Posed in another way: when would it not be justified to keep variations of the density only when they are coupled to the external gravity?

In Sec. II, an order of magnitude analysis is done in order to determine the relative importance of the baroclinic effects. The analysis places on firmer ground the conditions under which the Boussinesq approximation would be valid, which is the case when

$$g \gg \delta U \bar{U}_z \quad \text{and } g \gg \delta U^2 k_\rho, \tag{1}$$

as well as $k \gg k_\rho$. Here the external gravitational field is g, k is the inverse of the horizontal disturbance wavelength, k_ρ is the inverse of the vertical scale of the background density variation, $\bar{U}_z$ is the magnitude of the background shear, and δU is the larger measure of either (i) the difference of the background flow far from either side of the density interface or (ii) c, the wavespeed of the disturbance in question. A consequential result that follows from these conditions and orderings is that $\mathcal{O}(\delta U^2 k^2) \sim \mathcal{O}(g k_\rho)$. In this sense we recover the usual understanding of the Boussinesq approximation (BA), namely that k_ρ may be taken to be small yet leaving $g k_\rho / (\delta U^2 k^2)$ an order 1 quantity.

It is worth reviewing what is meant when one says that the TG equation neglects so-called baroclinic effects. Baroclinic torques are exerted, in general, when the flow exhibits properties such that at any time

$$T_f = \frac{1}{\rho^2} \nabla p \times \nabla \rho \neq 0,$$

where p and ρ, respectively, denote pressure and density. In linearized flow, the above expression contributes two terms to the baroclinic torques. In other words, if $\bar{p}, \bar{\rho}$ represent a "steady" configuration of an atmosphere while p', ρ' represent the conjoining linearized disturbances, then the baroclinic expression above becomes, to linear order,

$$\frac{1}{\bar{\rho}^2} \nabla \bar{p} \times \nabla \rho' + \frac{1}{\bar{\rho}^2} \nabla p' \times \nabla \bar{\rho},$$

where it is assumed that the steady configuration of the atmosphere is barotropic. If the basic state of the atmosphere is dominantly characterized by a hydrostatic balance, then the first term is associated with buoyancy effects and this is usually included in typical analyses. The second term, which is often times referred to as *baroclinic effects*, is what is discarded via the Boussinesq approximation and in the TG equation.

It is therefore our intention here to revisit the problem of Holmboe's normal mode instability and to ask how the inclusion of baroclinic effects alters the resulting dynamical activity. We approach this by solving the inviscid incompressible flow equations together with the equation of continuity. Instead of combining the linearized set into one master equation and then doing the usual matching procedures reserved for problems with discontinuities, we will begin instead from the primitive equations (having been linearized) and apply the solution procedure in the usual way (e.g., as in Chandrasekhar[14]). We find that Holmboe modes lose much of their symmetric properties since their propagation speeds and growth rates become dependent upon which direction the modes are moving. We also notice some other minor features. Holmboe's original problem does not limit to the Kelvin-Helmholtz result in the limit where the layer thickness goes to zero. In the problem of a globally constant shear profile with a single density interface, it is found that the usual Rayleigh-Taylor instability is suppressed at sufficiently long length scales when the baroclinic effects are included. In other words, shear appears to play a stabilizing role in this case.

This paper is organized as follows. In Sec. II, we formulate the linearized problem. We review the scaling argument justifying the use of the classical TG equations and consider the conditions in which inclusion of the baroclinic terms may be necessary, leading to the validity statement (1). We continue in Sec. III to solve what we call the *baroclinic Holmboe* problem, that is, Holmboe's problem without the Boussinesq assumption. We describe the normal mode solution to the generalized Holmboe basic state in an unbounded domain. In Sec. III A, we demonstrate its limiting forms to certain classical problems and their normal modes, namely (i) the Kelvin-Helmholtz solution, (ii) Rayleigh's 1880 solution, and (iii) Holmboe's classic problem. We review how these normal modes owe their origins to modes otherwise associated with the continuous spectrum. In Sec. III B, we present and discuss the problem of a globally constant shear with a density interface, followed in Sec. III C by a discussion of the baroclinic Holmboe problem. The first of these three subsections serves to review previous work in order to set the context within which the new results reside, with insights presented in the latter two subsections. In Sec. IV, we (a) review our results, (b) discuss the physical regime in

which the inclusion of these baroclinic effects may be important and assess whether they are relevant to known observations and experiments, and (c) compare and contrast the physical implications of the baroclinic effects as well as discuss future directions. The two appendixes detail the calculation performed.

II. FORMULATION OF THE BAROCLINIC TG EQUATION

The analysis of this study is restricted to two-dimensional disturbances. The flow is incompressible everywhere. We assume that there exists a background basic flow state in the horizontal ($\hat{\mathbf{x}}$) direction where its functional dependence is denoted by $\bar{U}(z)$, also implying its dependence on the vertical coordinate, z. The quantities u and v represent, respectively, the horizontal and vertical velocities atop the basic flow state $\bar{U}$. We assume no viscosity. The flow is in a constant gravitational field (g) pointing downward in the horizontal direction, $\mathbf{z}$. The total density is represented in two parts, one denoting the steady background state only dependent on z, i.e., $\bar{\rho}(z)$, and the other representing dynamical departures from this state, $\rho(x,z,t)$. Thus the full equations of motion are

$$\partial_x u + \partial_z v = 0, \tag{2}$$

$$(\partial_t + \bar{U}\partial_x + u\partial_x + v\partial_z)u + v\bar{U}_z = -\frac{\partial_x P}{\bar{\rho}+\rho}, \tag{3}$$

$$(\partial_t + \bar{U}\partial_x + u\partial_x + v\partial_z)v = -\frac{\partial_z \bar{P} + \partial_z P}{\bar{\rho}+\rho} - g, \tag{4}$$

$$(\partial_t + \bar{U}\partial_x + u\partial_x + v\partial_z)\rho + v\bar{\rho}_z = 0. \tag{5}$$

The pressure is broken up into its steady component $\bar{P}$ and its corresponding dynamical departure P. Hydrostatic balance relates $\bar{P}$ and $\bar{\rho}$,

$$\bar{P}_z = -g\bar{\rho}. \tag{6}$$

Linearization of the governing dynamical equations around this steady state reveals the following:

$$\partial_x u + \partial_z v = 0, \tag{7}$$

$$(\partial_t + \bar{U}\partial_x)u + v\bar{U}_z = -\frac{1}{\bar{\rho}}\partial_x P, \tag{8}$$

$$(\partial_t + \bar{U}\partial_x)v = -\frac{1}{\bar{\rho}}\partial_z P - g\frac{\rho}{\bar{\rho}}, \tag{9}$$

$$(\partial_t + \bar{U}\partial_x)\rho + v\bar{\rho}_z = 0. \tag{10}$$

Because the flow is incompressible, we may express the disturbance quantities in terms of a stream function ψ, that is,

$$v = -\partial_x \psi, \quad u = \partial_z \psi. \tag{11}$$

Additionally, we can consider the *vorticity* defined to be

$$\omega = \partial_z u - \partial_x v = (\partial_x^2 + \partial_z^2)\psi. \tag{12}$$

With these definitions in mind, the equations of motion may be cast into a single equation for the stream function ψ. One proceeds by (i) operating on (8) with ∂_z, (ii) operating on (9) with ∂_x, and (iii) subtracting the result leaving

$$(\partial_t + \bar{U}\partial_x)\omega + v\bar{U}_{zz} = \frac{\bar{\rho}_z}{\bar{\rho}}\left(\frac{1}{\bar{\rho}}\partial_x P\right) - g\partial_x\left(\frac{\rho}{\bar{\rho}}\right),$$

where the incompressibility condition was invoked. The above expression may then be further reduced by (iv) explicitly replacing the pressure term [the first term on the right-hand side (RHS)] with the relationship (8), (v) operating the resulting expression with $\partial_t + \bar{U}\partial_x$, and (vi) replacing the resulting last term on the RHS of the expression with the relationship in (10). Lastly, the velocity expressions are replaced according to their stream-function representation (11) to reveal the following:

$$(\partial_t + \bar{U}\partial_x)^2(\partial_z^2 + \partial_x^2)\psi - \bar{U}_{zz}(\partial_t + \bar{U}\partial_x)\partial_x\psi - \frac{\bar{\rho}_z}{\bar{\rho}}g\partial_x^2\psi + \frac{\bar{\rho}_z}{\bar{\rho}}[(\partial_t + \bar{U}\partial_x)^2\partial_z\psi - \bar{U}_z(\partial_t + \bar{U}\partial_x)\partial_x\psi] = 0. \tag{13}$$

The Taylor-Goldstein equation is (13) with the terms involving the variation of the density coupled to the advective-inertial terms neglected,[15,16] i.e.,

$$(\partial_t + \bar{U}\partial_x)^2(\partial_z^2 + \partial_x^2)\psi - \bar{U}_{zz}(\partial_t + \bar{U}\partial_x)\partial_x\psi - \frac{\bar{\rho}_z}{\bar{\rho}}g\partial_x^2\psi = 0. \tag{14}$$

Inspection of the baroclinic terms dropped from (13) leads one to ask the following: How might the baroclinic effects modify or shape the linearized dynamics in systems of the sort considered here? In particular, we note that these neglected baroclinic terms are proportional to $\bar{\rho}_z/\bar{\rho}$ just as the retained buoyancy term. This observation suggests that one ought to be able to formulate a firm scaling argument declaring better the conditions under which the buoyancy term dominates the baroclinic term. Such a statement will provide a condition for the validity of the Boussinesq approximation and ultimately the TG equation. Such an analysis is presented below.

As (13) is the exact linearized formulation of these equations of motion, one may consider normal mode solutions of the form

$$\psi = \hat{\psi}(z)e^{ik(x-ct)} + \text{c.c.},$$

and if we let λ_ρ be the atmosphere's *scale height* and have it be defined by the expression

$$\frac{1}{\lambda_\rho} = k_\rho \equiv \frac{\bar{\rho}_z}{\bar{\rho}},$$

then (13) becomes

$$\left[\partial_z^2 + k_\rho \partial_z - k^2 - \left(\frac{k_\rho \bar{U}_z + \bar{U}_{zz}}{\bar{U}-c}\right) - \frac{g k_\rho}{(\bar{U}-c)^2}\right]\hat{\psi} = 0, \quad (15)$$

cf. Eq. (44.7) of Drazin and Reid.[15] By contrast, the Taylor-Goldstein equation (14) with the normal-mode ansatz is rewritten as

$$\left[\partial_z^2 - k^2 - \left(\frac{\bar{U}_{zz}}{\bar{U}-c}\right) - \frac{g k_\rho}{(\bar{U}-c)^2}\right]\hat{\psi} = 0. \quad (16)$$

Note that it is common in the literature to designate $\mathcal{J}(z) = -k_\rho g$ as the square of the Brunt-Väisälä frequency.[15] Following Taylor,[1] we define a modified stream function,

$$\hat{\psi} \equiv \frac{\hat{\Psi}}{\sqrt{\bar{\rho}}},$$

and introduce it into (15) to find

$$\left[\partial_z^2 - \frac{1}{4}k_\rho^2 - k^2 - \frac{1}{2}\frac{\partial k_\rho}{\partial z} - \left(\frac{\bar{U}_z k_\rho + \bar{U}_{zz}}{\bar{U}-c}\right) - \frac{g k_\rho}{(\bar{U}-c)^2}\right]\hat{\Psi} = 0. \quad (17)$$

First implicit in the BA is the assumption that the horizontal length scales are much shorter than the vertical variation of the background density gradient. In other words, the BA assumes that $k \ll k_\rho$.

An analysis of the importance of the baroclinic effect may be best considered by studying its role in (17). The often neglected term,

$$\frac{k_\rho \bar{U}_z}{\bar{U}-c} \sim \mathcal{O}\left(\frac{k_\rho \bar{U}_z}{\delta U}\right), \quad (18a)$$

must be considered against the classical buoyancy term,

$$\frac{g k_\rho}{(\bar{U}-c)^2} \sim \mathcal{O}\left(\frac{g k_\rho}{\delta U^2}\right). \quad (18b)$$

The scalings appearing after each expression above are justified by noticing (see the review of the classic Holmboe analysis below) that the resulting wave speeds, in the small horizontal wavenumber limit, are such that $\bar{U}-c$ is the greater of either (i) the magnitude of the difference of the two background flow speeds far from the interface, $|U_+ - U_-|$, where $U_\pm = U(z \to \pm\infty)$,[19] or (ii) the buoyancy wave speed $\sqrt{\delta\rho g/k}$, where k is the disturbance wavenumber and where $\delta\rho \equiv (\rho_+ - \rho_-)/(\rho_+ + \rho_-)$ is similarly a scaled magnitude measure of the difference in densities far from either side of the shear interface. In other words, we assume that $\delta U = \mathcal{O}(|U_+ - U_-|, \sqrt{\delta\rho g/k})$, where the choice of these will depend upon which mode is being considered. We note again that these cited scalings are asymptotically correct in the small wavenumber limit [for example, see the asymptotic forms in Eq. (34)].

Neglecting the baroclinic term while keeping the buoyancy term constitutes the BA. In the classical vernacular with respect to this matter, the BA amounts to saying that variations of the density are only considered when coupled to the external gravity. A scaling argument leading to the BA is to say the following: one may let the background density gradient go to zero, i.e., $k_\rho \to 0$, yet have the gravity go to infinity, i.e., $g \to \infty$, in such a way that the product of the two terms remains an order 1 quantity. It follows from this construction that those terms involving k_ρ that are not coupled to gravity are then always subdominant to the buoyancy term.

By comparing the two terms of (18b) and (18b), i.e., $\delta U \bar{U}_z \cdot k_\rho$ and $g \cdot k_\rho$, the limiting procedure just outlined is really saying that the BA is appropriate for use when

$$\mathcal{O}(g) \gg \mathcal{O}(\delta U \bar{U}_z). \quad (19)$$

In other words, the BA $\delta U \bar{U}_z$ is always a "small" acceleration compared to g. However, in those cases in which the shear transition layer is made infinitely small (making $\bar{U}_z$ correspondingly large) and/or when the disturbance wavenumber is small (making $\delta U \sim 1/\sqrt{k}$), the assumed dominance of g over $\delta U \bar{U}_z$ will break down. As the infinitely thin shear layer configuration is approached, as one must affect in order to reach the Kelvin-Helmholtz limit, the assumed asymptotic dominance of g over $\delta U \bar{U}_z$ (taken as axiomatic in the BA) must break down. *In addition, this analysis suggests that disturbances involving long wavelengths should lead to some qualitative differences if the BA is assumed in the consideration of Holmboe modes.*

Finally, in order to technically complete the scaling analysis justifying the BA, one must also require that

$$\mathcal{O}(k_\rho^2) \ll \mathcal{O}\left(\frac{g k_\rho}{\delta U^2}, \frac{\bar{U}_z k_\rho}{\delta U}\right), \quad (20)$$

however, given the dominance implied by (19), the above requires that

$$\mathcal{O}(k_\rho) \ll \mathcal{O}\left(\frac{g}{\delta U^2}\right). \quad (21)$$

It follows then that those terms that remain would imply that

$$\mathcal{O}(k^2) \sim \mathcal{O}\left(\frac{g k_\rho}{\delta U^2}\right). \quad (22)$$

Consequently *in nondimensionalized units*, if $\mathcal{O}(\delta U^2 k^2) \sim \mathcal{O}(1)$, then it follows that $\mathcal{O}(g k_\rho) \sim \mathcal{O}(1)$ as well. This is nothing but the classical justification of the BA, namely that k_ρ may be taken as small as one likes yet leaving the product $g k_\rho$ an order 1 quantity.

III. THE BAROCLINIC HOLMBOE PROBLEM: A CASE STUDY WITH DISCONTINUITIES

We consider an infinite vertical domain split in half by fluids of two different densities at $z=0$, that is (see Fig. 2),

$$\bar{\rho} = \begin{cases} \rho_0 - \frac{1}{2}\delta, & z > 0, \\ \rho_0 + \frac{1}{2}\delta, & z < 0. \end{cases} \quad (23)$$

We use a nondimensional measure of the density difference between these layers by defining

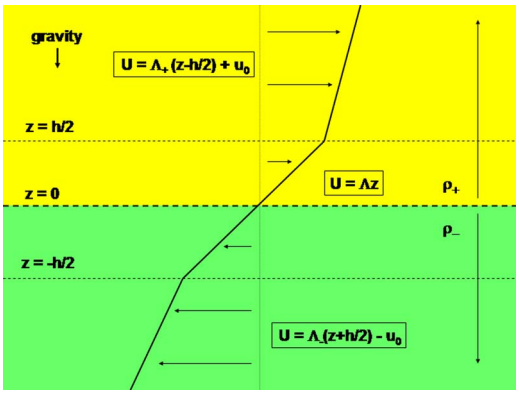

FIG. 2. (Color online) A schematic for a generalization of Holmboe's problem.

$$\Delta \equiv \frac{\delta}{\rho_0}.$$

Note that the values Δ can take are restricted according to $-2<\Delta<2$. In steady state, solutions of the hydrostatic equilibrium relation give

$$\bar{P} = \begin{cases} -\rho_0\left(1-\frac{1}{2}\Delta\right)gz + \bar{P}_0, & z>0, \\ -\rho_0\left(1+\frac{1}{2}\Delta\right)gz + \bar{P}_0, & z<0, \end{cases} \tag{24}$$

where $\bar{P}_0$ is a constant whose value is the pressure at $z=0$. Note that the pressure here is continuous, although its vertical gradient has a discontinuity at $z=0$.

For the sake of illustration, we consider a velocity profile composed of several constant shear layers of the sort,

$$\bar{U} = \begin{cases} \Lambda_+\left(z-\frac{h}{2}\right) + \Lambda\frac{h}{2}, & z>\frac{h}{2}, \\ \Lambda z, & -\frac{h}{2}<z<\frac{h}{2}, \\ \Lambda_-\left(z+\frac{h}{2}\right) - \Lambda\frac{h}{2}, & z<-\frac{h}{2}, \end{cases} \tag{25}$$

where $\Lambda, \Lambda_\pm$ are constants. Inspection of the above shows that $\bar{U}$ is continuous across the domain while the shear, $\bar{U}_z$, is step-like. The shear constant Λ is related to the fiducial velocities at the positions $z=\pm h/2$ by identifying $\Lambda=u_0/h$. That means that $\bar{U}(\pm h/2)=\pm u_0/2$. Another nondimensional quantity in common use in the literature[18] is to define J, the *Richardson number*, as

$$J \equiv \Delta\frac{gh}{u_0^2},$$

which is a measure of the effect of buoyancy versus shear. We refer to this configuration as the *generalized Holmboe basic state.*

The general normal mode calculation is straightforward and its details (along with a procedural review) are presented in Appendixes A and B. What results is a fourth-order dispersion problem for the complex wavespeed c, i.e.,

$$c^4 + a_1c^3 + a_2c^2 + a_3c + a_4 = 0, \tag{26}$$

where the general forms for the constants a_i are given in Appendix B. In this study, we will consider only special cases dictated, for instance, by the constants $\Lambda_\pm$ and limiting values of J and Δ and the nondimensionalized wavenumber $K \equiv kh$.

We set the scene for what follows by noting that the basic tenets of the Taylor-Goldstein ansatz is equivalent to the Boussinesq assumption. As in standard studies of buoyant convection,[14] the Boussinesq assumption, aside from incompressibility, is to suppress density variations of any sort (both steady and dynamical) except for when they couple to gravity. In the way the problem has been formulated, the Boussinessq/TG limit is mathematically recovered by setting the density variation term to zero, i.e., $\Delta=0$, while maintaining the Richardson number to be nonzero (i.e., $J\neq 0$).

A. Classic limits

1. $h\to 0$, $\Lambda_\pm=0$: Kelvin-Helmholtz limit

It is natural to verify that this theory is limited to the results of the Kelvin-Helmholtz (KH) problem in the limit in which the separation of the two layers goes to zero. First, we begin by setting $\Lambda_\pm=0$, which recovers the usual Rayleigh problem configuration. Second (and this is done frequently throughout the remainder of this work), Λ is rewritten according to $\Lambda=u_0/h$. Because according to the definitions of K and J, namely that each is linearly proportional to the separation h, the Kelvin-Helmholtz limit is achieved by taking the limit of (26) for

$$K\to 0, \quad J\to 0, \quad \text{while } \frac{J}{K}\neq 0. \tag{27}$$

In practice, it means assuming K to be small and appropriately Taylor-expanding the expressions for a_i in (B11a)–(B11d). The dispersion relation simplifies to

$$c^2\left(c^2 + \frac{\Delta u_0}{2}c - \frac{g\Delta}{2k} + \frac{u_0^2}{4}\right) + \mathcal{O}(h) = 0. \tag{28}$$

Aside from the two null roots, the remaining pair of wavespeeds is, after restoring dimensional quantities,

$$c = \frac{\rho_+\bar{U}\left(\frac{h}{2}\right) + \rho_-\bar{U}\left(-\frac{h}{2}\right)}{\rho_+ + \rho_-} \pm \left[\frac{g}{k}\left(\frac{\rho_- - \rho_+}{\rho_+ + \rho_-}\right) - \frac{\rho_+\rho_-\left[\bar{U}\left(\frac{h}{2}\right) - \bar{U}\left(-\frac{h}{2}\right)\right]^2}{(\rho_+ + \rho_-)^2}\right]^{1/2}, \tag{29}$$

in which we have employed the definitions $\rho_\pm=\rho_0\left(1\mp\frac{1}{2}\Delta\right)$, which were used in Appendix B. The above expression compares exactly with the expression for the wavespeed for the Kelvin-Helmholtz problem [cf. Eq. (4.20) in Drazin and Reid[7]]. Although this is well known, we remind the reader that an inspection of the terms under the radical sign in (29) shows that the Kelvin-Helmholtz result predicts that shear,

manifesting itself here as a discontinuous jump in the horizontal flow, is a destabilizing agent for disturbances.

2. $\Delta = J = 0$: Rayleigh's 1880 and case 1960

When there is no gravity and no density jumps anywhere, the results reduce to the problem first investigated by Rayleigh[4] (see also Sec. 23.2 in Drazin and Reid[15]). Setting $\Lambda_\pm = 0$ recovers the profile he assumes. The physical problem and its corresponding dispersion relation, which are frequently interpreted in terms of counterpropagating Rossby waves,[13] is

$$c^4 - \frac{u_0^2}{4K^2}[(K-1)^2 - e^{-2K}]c^2 = 0. \tag{30}$$

Besides the null modes, the remaining pair of solutions are

$$c = \pm \frac{u_0}{2kh}[(kh-1)^2 - e^{-2kh}]^{1/2} = 0.$$

Modes in this unbounded shear layer are well known to become exponentially growing when $(K-1)^2 - e^{-2K} < 0$.

It is known that the problem involving an infinitely extended constant shear (in 2D) has no normal-mode solution, although there are initial value solutions comprised of a continuous spectrum.[17] It is instructive to examine here what happens under those circumstances by setting $\Lambda_\pm = \Lambda$ in (B10) giving

$$c^4 - \frac{u_0^2}{4}c^2 = 0. \tag{31}$$

In addition to the double $c=0$ root, this dispersion relation also predicts two wavespeeds of $c = \pm u_0/2$, corresponding exactly to the background flow speed at the respective positions $z = \pm h/2$ of the shearing fluid. Whereas a classical (global) normal-mode analysis admits no normal modes for this problem, there are two nonzero normal modes predicted here with zero amplitude. This can be interpreted as being a manifestation of the continuous spectrum. On either side of each of the discontinuities, one observes no difference in the background shear. Consequently, one expects there to be no effective perturbation vorticity generation since, for example, an Eulerian observer will measure the same total vorticity, in contrast to the classical Taylor problem ($\Lambda_\pm = 0$) in which an Eulerian observer will measure step-function changes of the vorticity as the front passes through this position. Because under these conditions there is no jump in vorticity, the discontinuities become "ghost"-like. As such, this classical analysis actually serves to capture a set of modes (here just two) that otherwise belong to the continuous spectrum. We call these "ghost-like" in this normal-mode analysis because they have zero amplitude according to (A2). These modes would be excited to nonzero amplitude in an initial-value problem investigation. If one considers disturbances about a set "ghost" discontinuities corresponding to the positions $z = \{z_i\}$ and if one repeats the same procedure, then one would predict a set of wavespeeds $c = \{c_i\} = \{\bar{U}(z_i)\}$.

3. $\Delta = \Lambda_\pm = 0$: A review of the classic Holmboe problem

As discussed in the Introduction, Holmboe's results are generated from assuming the Taylor-Goldstein equation in the Rayleigh flow geometry, i.e., $\Lambda_\pm = 0$. At the heart of the Taylor-Goldstein ansatz lies the assumption, shared by the basic Boussinesq approximation, that density differences are dynamically significant only when they are coupled to gravity. In the way the problem has been formulated in this study, the TG ansatz is realized by setting $\Delta = 0$ while keeping $J \neq 0$. Indeed, this procedure reduces the dispersion relation (26) to

$$c^4 - \left(\frac{u_0}{2K}\right)^2 [2JK + (K-1)^2 - e^{-2K}]c^2 + 2JK\left(\frac{u_0}{2K}\right)^4 [K - 1 + e^{-K}]^2 = 0. \tag{32}$$

Careful inspection of (32) shows it to be equivalent to Holmboe's equation [cf. Eq. (4) of Lawrence *et al.*[18]]. The general stability characteristics of this equation are well known[17] and we briefly summarize them here. If $(K-1)^2 + 2JK - e^{-2K} > 0$ as well as $J > 0$, then all four disturbances oscillate with no growth or decay. If $(K-1)^2 + 2JK - e^{-2K} > 0$ and $J < 0$, then there is one pair of oscillating modes and a pair of growing/decaying exponential modes. These unstable modes are related to the Rayleigh-Taylor instability (that is, for an unstable density stratification). If $(K-1)^2 + 2JK - e^{-2K} < 0$ and $J < 0$ again, there is one pair of growing/decaying exponential modes and another pair of oscillating modes that are similarly associated with the Rayleigh-Taylor instability.

The Holmboe instability, namely the appearance of two pairs of complex conjugate modes, i.e., modes where $c = \pm c_r \pm i c_i$ with $c_r, c_i \in \mathcal{R}^+$, occurs if $J^{(+)} > J > J^{(-)}$, in which $J^{(\pm)}$ is the solution to the condition

$$[(K-1)^2 + 2JK - e^{-2K}]^2 - 8JK[(K-1) + e^{-K}]^2 < 0.$$

Its solution is

$$J^{(\pm)} = \frac{e^{-2K}}{2K}\{3 + e^K(K-1)[4 + e^K(K-1)]\} \pm \frac{e^{-2K}}{K}\{2[1 + e^K(K-1)]^3\}^{1/2}. \tag{33}$$

In the language used by Lawrence *et al.*,[10] the $+/-$ modes are referred to as the *positive/negative instability*. Inspection of the stability of the critical Richardson numbers above shows that Holmboe modes do not exist for values of $J < 0$. In other words, both $J^{(\pm)} > 0$.

If $(K-1)^2 + 2JK - e^{-2K} < 0$, then there is a region bounded by $J^{(-)} > J > 0$ in which there are two pairs of exponentially growing/decaying modes that we will refer to as *nonpropagating double instabilities*. One pair of these *nonpropagating* modes is associated with the Rayleigh unbounded shear layer instability (i.e., the instability when $J = 0$ of the previous section). With the help of Figs. 3 and 4, we may summarize the salient qualitative features of Holmboe's results for $J > 0$. The dispersion curves are shown for the complex frequency defined by

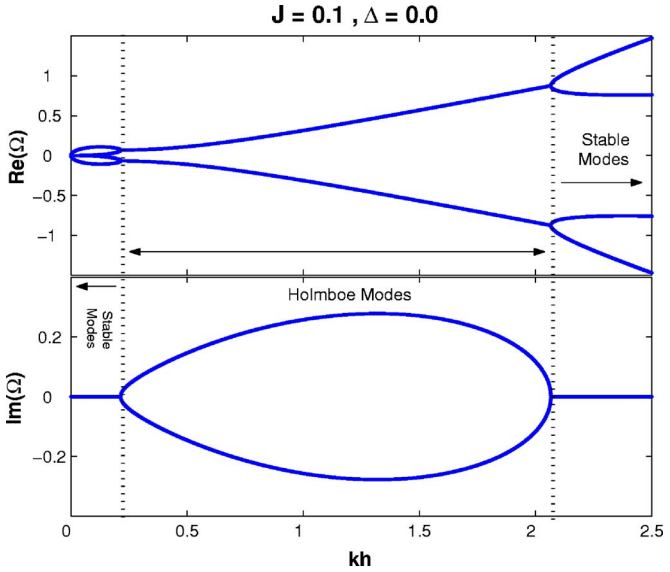

FIG. 3. (Color online) Dispersion relationship for the classic Holmboe problem with $\Delta=0$ and $J=0.1$. The appearance of Holmboe modes occurs in a range in K between 0.2 and 2. Note that the wavespeeds and growth rates of the four modes have the form $c=\pm c_r \pm i c_i$.

$$\Omega \equiv \frac{2Kc}{u_0}.$$

The transition from Holmboe-type modes to stable modes occurs when the real wavespeeds of Holmboe modes bifurcate. We indicate in Fig. 5 those regions in parameter space supporting the various types of modes.

Further analysis shows that in the limit in which $K \to 0$, the four modes have the asymptotic form

$$c^2 = \frac{u_0^2 J}{2K} + \mathcal{O}(K) \quad \text{and} \quad c^2 = \frac{u_0^2}{16}K^2 + \mathcal{O}(K^4). \tag{34}$$

Holmboe's result, i.e., the general dispersion relation (32), is unable to limit to the Kelvin-Helmholtz problem as $h \to 0$. To best illustrate this, we apply the limiting process prescribed by (27)–(32). We find the resulting dispersion relation,

$$c^2\left(c^2 - \frac{g\Delta}{2k} + \frac{u_0^2}{4}\right) + \mathcal{O}(h) = 0. \tag{35}$$

As $h \to 0$, the nontrivial solution for the wavespeed becomes (after restoring dimensional quantities)

$$c = \pm\left[\frac{g}{k}\left(\frac{\rho_- - \rho_+}{\rho_+ + \rho_-}\right) - \frac{u_0^2}{4}\right]^{1/2}, \tag{36}$$

which is not the classic KH limit (29) but is, instead, the Boussinesq-Kelvin-Helmholtz (BKH) result. There are two differences between these results. The first is that the classic Kelvin-Helmholtz analysis predicts that there will be a propagation speed for the modes that are unstable and this speed is associated with the center-of-mass reference frame. The BKH result, on the other hand, predicts that those modes that are unstable appear stationary in the laboratory frame. The second difference is that the predicted growth rates are different despite the center-of-mass reference frame shift. Moving into such a frame with respect to the KH result, (29),

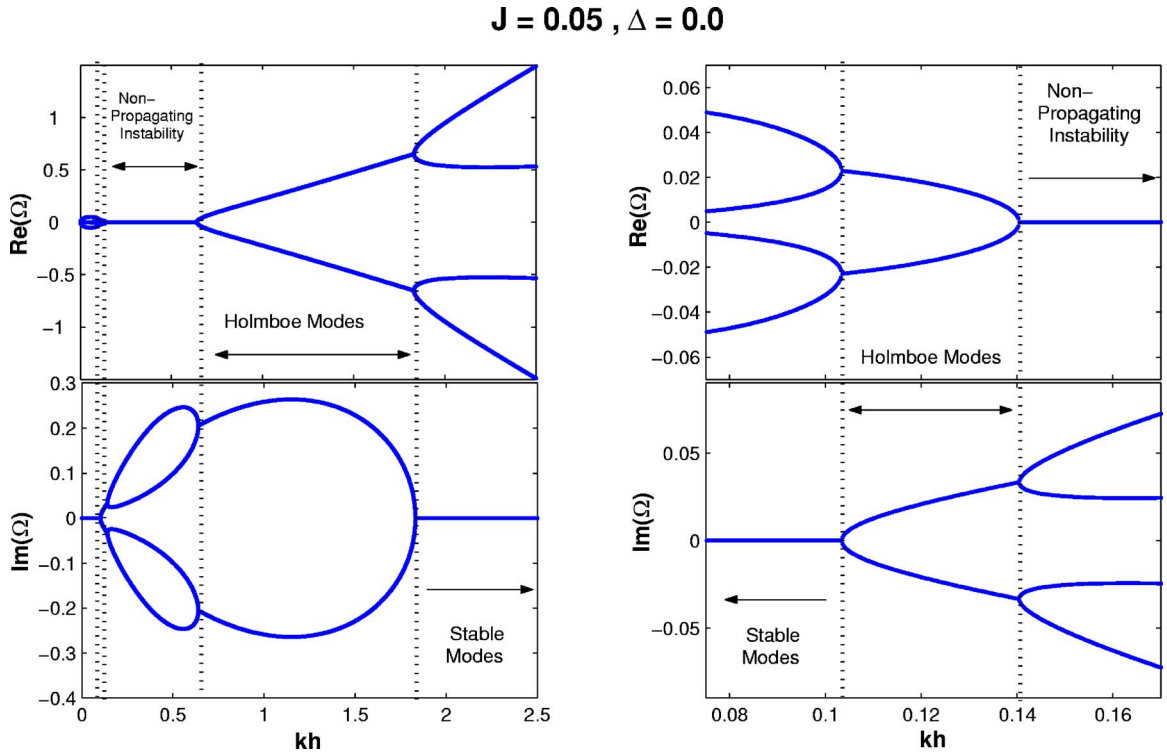

FIG. 4. (Color online) Dispersion relationship for the classic Holmboe problem with $\Delta=0$ and $J=0.05$. Unlike in Fig. 3, there are now two ranges in K in which Holmboe modes exist. The right panel is a blowup view near $K=0.1$ detailing the appearance of this second Holmboe mode range. Additionally, the two Holmboe mode ranges sandwich a range in K between 0.14 and 0.63 supporting two pairs of nonpropagating exponentially growing/decaying modes.

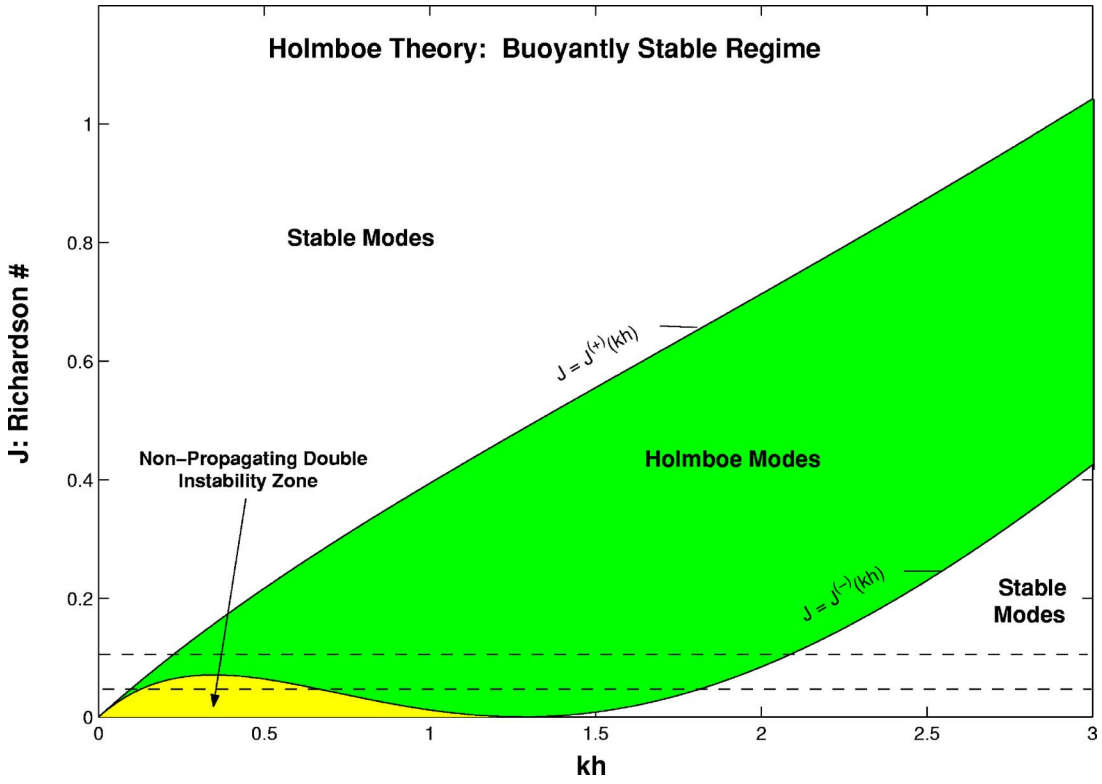

FIG. 5. (Color online) A summary of Holmboe mode theory. The Holmboe mode boundaries are shown between the shaded regions bounded by the curves $J^{(\pm)}(kh)$. The nonpropagating double instability zone is the region $0<J<J^{(-)}$ lying in the range $0<K<1.278$. Also displayed with horizontal dashed lines is the cut in parameter space corresponding to the dispersion relations depicted in Figs. 3 and 4.

and after replacing terms one finds that the KH growth rate, $\mathrm{Im}(c_{\mathrm{KH}})$, may be written as

$$\mathrm{Im}(c_{\mathrm{KH}}) = \left[\frac{g\Delta}{2k} + \left(1 - \frac{\Delta^2}{4}\right)\frac{u_0^2}{4}\right]^{1/2}. \tag{37}$$

By taking a ratio of this to the BKH growth rate, $\mathrm{Im}(c_{\mathrm{BKH}})$ shows that

$$\frac{\mathrm{Im}(c_{\mathrm{KH}})}{\mathrm{Im}(c_{\mathrm{BKH}})} = \frac{\left[1 + \left(1 - \frac{\Delta^2}{4}\right)\frac{u_0^2}{2g\Delta}k\right]^{1/2}}{\left[1 + \frac{u_0^2}{2g\Delta}k\right]^{1/2}} < 1. \tag{38}$$

Inspection of this expression shows that the BKH result will slightly overpredict the growth rate in this instance. The baroclinic effects here, controlled by the expression $\Delta^2/4$, reduce the predicted growth rates. The effect is more pronounced as Δ is made larger.

B. $\Lambda_{\pm}=\Lambda$: Globally constant shear flow with a density interface

By setting $\Lambda_{\pm}=\Lambda$, the flow configuration simplifies to that of a globally constant shear profile (a shear layer of "infinite" width) punctuated by a density interface at $z=0$ (see Fig. 6 for a schematic). The dispersion relation simplifies greatly to

$$\left(c^2 - \frac{u_0^2}{4}\right)\left(c^2 + \frac{\Delta}{2K}u_0 c - \frac{J}{2K}u_0^2\right) = 0. \tag{39}$$

There are two modes that represent disturbances propagating with the local velocities at $z=\pm h/2$, that is, $c=\bar{U}(\pm h/2) = \pm u_0/2$. As already discussed, these two modes are members of the continuous spectrum. On the other hand, the remaining two modes represent shear modified Rayleigh-Taylor type disturbances,

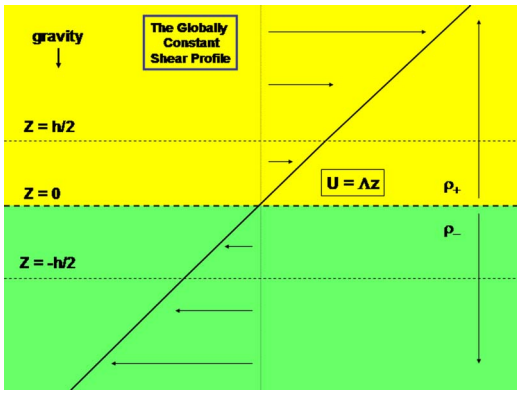

FIG. 6. (Color online) Infinite shear layer schematic.

$$c = -\frac{\Lambda}{2k}\left(\frac{\rho_- - \rho_+}{\rho_- + \rho_+}\right) \pm \frac{1}{2}\left[\frac{g}{k}\left(\frac{\rho_- - \rho_+}{\rho_+ + \rho_-}\right) + \frac{\Lambda^2}{k^2}\left(\frac{\rho_- - \rho_+}{\rho_- + \rho_+}\right)^2\right]^{1/2}. \tag{40}$$

In contrast to the KH modes [see (29)], the dispersion solution (40) says that a smooth shear behaves as a stabilizing agent to these kinds of disturbances since the shear term under the radical sign is always positive definite, as opposed to the corresponding analogous term in (29). Buoyancy is a dominating effect for sufficiently small wavelength disturbances. What is most surprising is that the dynamical stability implied by shear dominates the destabilizing role of unstable buoyant modes for sufficiently long length scale disturbances. In particular, the marginal condition under the radical sign indicates the critical transition which occurs for wavenumbers that satisfy

$$0 \leqslant k < k_c = \frac{\Lambda^2}{16g}\left(\frac{\rho_+ - \rho_-}{\rho_+ + \rho_-}\right), \tag{41}$$

which holds only for configurations where $\rho_+ - \rho_- > 0$, that is, in an otherwise statically unstable configuration since otherwise there is no instability. Because there is no natural length scale in the shear, the corresponding characteristic scale (ℓ) at which this type of shear profile is dynamically significant over buoyant dynamics is when $\ell \sim g/\Lambda^2$.

It is important to rationalize on some level the differences inherent in the typical KH instability and the instability according to the Boussinesq formalism. In particular, had the problem of the globally constant shear been treated according to the Boussinesq ansatz, namely by setting $\Delta = 0$ and $J \neq 0$ in (39), we would find that the dispersion relation is that of the classic Rayleigh-Taylor instability, i.e.,

$$c = \pm \frac{1}{2}\left[\frac{g}{k}\left(\frac{\rho_- - \rho_+}{\rho_+ + \rho_-}\right)\right]^{1/2}. \tag{42}$$

The implication of this result is to say that an analysis of disturbances of a density interface with a globally constant shear, done with the Boussinesq assumption, will *miss any dynamical influence that shear will have on the disturbances*. This means that the resulting normal modes behave as if there were no shear at all.

The physical reason for this total absence lies in where the Boussinesq assumption is made. In terms of the horizontal momentum balance equations, the density on either side of the interface would be taken to be the same under the Boussinesq ansatz; cf. (A6). The densities appropriate to whichever side of the interface one is on, i.e., $\rho_\pm$, would be replaced instead by some average density (say $\bar{\rho}_0$). This means that the aggregate horizontal momentum fluxes due to the basic shear, both above and below the density interface, would be equal and opposite. As a result, the shear would exert no dynamical influence in the resulting stress condition (A5) since, by construction, those terms associated with the shear will cancel out exactly. Furthermore, waves traveling toward either direction feel/exert no net momentum transfer from/to the fluid as a result of their propagation.

When the Boussinesq ansatz is relaxed, then there exists an asymmetry between the left- and right-going waves because there is a net transfer of momentum (in the basic state) by the shear/density profile. Ultimately this shows up as an asymmetry in the respective propagation wavespeeds, i.e., the first term on the RHS of (40) represents a sort of "center-of-mass frame" of the flow. From the vantage point of this moving frame, waves appear to propagate symmetrically.

C. $\Lambda_\pm = 0$, the baroclinic Holmboe problem

In this more general case, the dispersion relationship becomes

$$c^4 + \Delta\left(\frac{u_0}{2K}\right)(1 - e^{-K})c^3 - \left(\frac{u_0}{2K}\right)^2[2JK + (K-1)^2 - e^{-2K}]c^2 - \Delta\left(\frac{u_0}{2K}\right)^3[K - 1 + e^{-K}]^2 c + 2JK\left(\frac{u_0}{2K}\right)^4[K - 1 + e^{-K}]^2 = 0. \tag{43}$$

It is best to discuss the effects of baroclinicity in contrast to the classic Holmboe analysis ($\Delta = 0$). The first very clear difference is that the introduction of baroclinicity breaks the left/right symmetry in the propagation speeds. In other words, the inclusion of baroclinic effects distinguishes between waves propagating leftward or rightward, unlike in the $\Delta = 0$ theory, where waves propagate with equal speed irrespective of direction (see Figs. 7 and 8).

The mechanical physics of this wavespeed asymmetry is related to the wave propagation properties in a globally constant shear flow (cf. Sec. III B).

Another subtle mathematical feature is that any nonzero amount of baroclinicity, i.e., $\Delta > 0$, wipes away the nonpropagating double instability zone discussed in terms of the classic Holmboe theory, and in its place appear four Holmboe modes, i.e., growing/decaying propagating modes. This is depicted in Fig. 9. In the classic theory, Holmboe modes appear in groups of four with wavespeeds $\pm c_r \pm c_i$. Bifurcation into or out of the Holmboe instability in parameter space occurs simultaneously as the relevant parameter is tuned (either K or J). For $\Delta > 0$, the bifurcation occurs first for the *positive instability* (cf. Sec. III A), i.e., modes propagating rightward. As the wavenumber $K = kh$ approaches the bifurcation point from the stable regime, the mode propagation speeds converge upon each other. Once converged, the modes become unstable and the propagation speeds become locked. Beyond this bifurcation point, there now exists a range of K where there are two Holmboe modes and two stable modes. As one moves toward even larger wavenumbers, the left-going waves (the negative instability) eventually bifurcate into existence in the same way described for the positive instability. Beyond the negative instability bifurcation point, there is now a window in K in which there are four Holmboe modes, just like in the $\Delta = 0$ theory. As K is continuously increased, however, the right-going waves find their growth/decay rates merging at 0; these two modes become stable and their propagation speeds unlock from each other. Beyond this value of K there are only the two left-

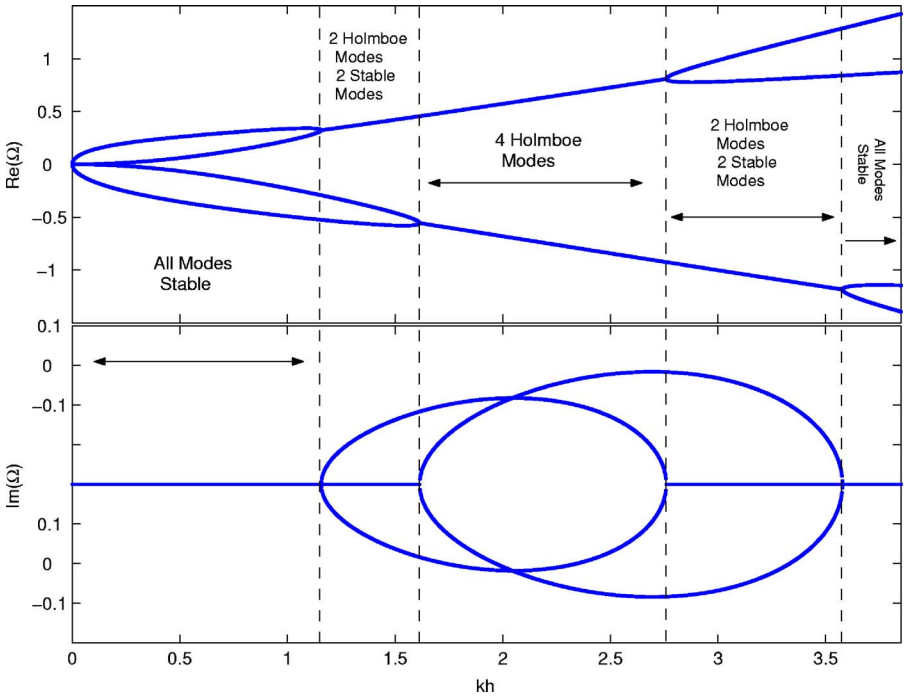

FIG. 7. (Color online) Dispersion relation $J=0.5$, $\Delta=0.5$.

propagating Holmboe modes. Just as before, the left-going waves follow suit: their growth/decay rates merge as K is increased, leaving behind two more stable modes with unlocked propagation speeds.

At given values of K and for extreme values of Δ and J, positive and negative instabilities do not necessarily coexist. In other words, as K is increased, the right-propagating Holmboe modes come into and out of existence before the left-propagating Holmboe modes do (see, e.g., Fig. 7 and the bottom panel of Fig. 8).

IV. DISCUSSION AND CONCLUSIONS

Because the TG equation assumes the Boussinesq approximation, its application is formally limited to physical scenarios that satisfy the assumptions underlying the approximation. Through a scaling argument and analysis of the exact governing equation, we have shown that the regime of validity is when (1) is satisfied. The question that seems natural to us is as follows: What would be the dynamical outcome to incompressible atmospheric flow problems in

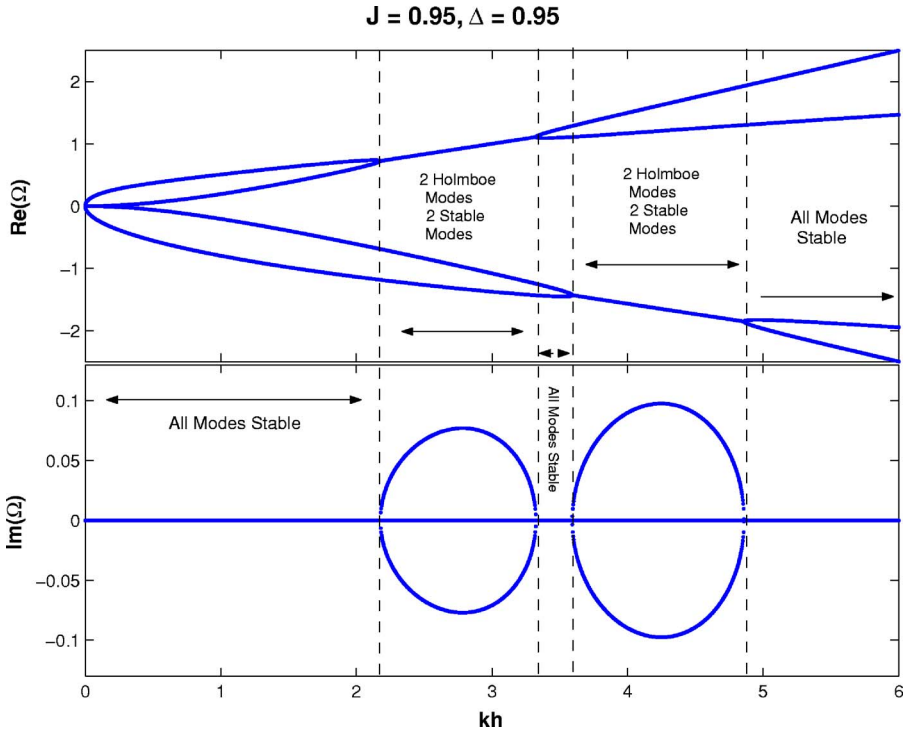

FIG. 8. (Color online) Dispersion relation $J=0.95$, $\Delta=0.95$.

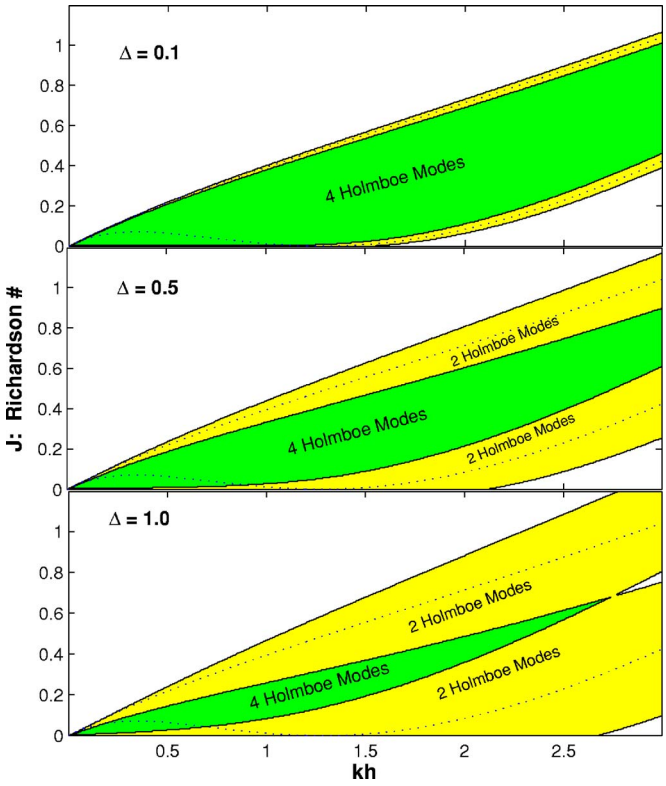

FIG. 9. (Color online) The stability regions for three values of Δ. The green zone signifies the presence of four Holmboe modes. The yellow zones indicate two Holmboe modes and two stable modes. The unshaded zones correspond to four stable modes. Also indicated by dashed curves is the stability boundaries given by $J^{\pm}$, i.e., the $\Delta=0$ theory (see Fig. 5). Note that the nonpropagating double instability zone of the $\Delta=0$ theory vanishes instantly when $\Delta>0$.

which (1) is violated. This question is equivalent to inquiring as to how baroclinic effects (i.e., those physical effects filtered out by the Boussinesq approximation) modify the dynamical outcome in such problems. In short, does a liberal application of the TG equation to problems whose basic states or dynamical responses violate the regime of validity of the Boussinesq ansatz (1) lead to dynamics that are significantly different from the predicted dynamics where baroclinic effects are formally included in the analysis?

In this sense, we consider the problem of Holmboe's instability to be a natural setting to pursue this question. In the context of that problem, the constraints implied by (1) suggest that the BA should formally break down with respect to the description of Holmboe modes when the horizontal wavelength of disturbances is sufficiently small (making c large) and/or if the size of the shear layer is narrow enough ($\bar{U}_z$ large).

This work has achieved some deeper insight into the modification of these modes by including baroclinic effects into a "generalized" Holmboe configuration (Fig. 2). The results show some notable differences in the normal-mode behavior compared to the classical results The problem has been crafted in such a way as to be governed by three parameters: the nondimensional measure of the density difference at the interface, Δ; the nondimensionalized wavenumber K, whose physical scale is measured by the layer thickness h; and the Richardson number J, which measures the buoyant time to the shear time. In the theory we have extended here, the Boussinesq limit (i.e., the TG ansatz) is achieved by keeping $J\neq 0$ while letting $\Delta\rightarrow 0$, and baroclinicity is measured by Δ.

The most important result we see implied by the normal-mode analysis is that the baroclinic influence breaks the symmetry of the classic Holmboe modes (reviewed in Sec. III A). By this we mean to say that both the complex wavespeeds and the incidence in parameter space for the rightward- and leftward-propagating Holmboe modes are now no longer the same. The source of this asymmetry can be found in the way momenta are matched across the discontinuous surfaces. In particular, the culprit appears to be the matching of the normal stresses across the moving surface: in the Boussinesq approximation, the horizontal fluxes [see (A6)] are calculated incorrectly because the densities across surfaces are taken to be the same (except when coupled to gravity) while in the correct treatment the difference in densities is preserved. In the more strict treatment, we find that the horizontal momentum fluxes *above and below* the density discontinuity are no longer equal and opposite as they are (by construction) in the Boussinesq approximation. This is the broken symmetry and its hand propagates throughout the resulting mode properties: propagation speeds are no longer equal and opposite, and the right- and left-propagating Holmboe modes are not locked to each other in parameter space as they are in Holmboe's classic treatment (e.g., see Figs. 7 and 8). There are some additional minor observations we have made:

(i) For a certain range in parameter space, Holmboe's classic theory predicts the existence of two pairs of exponential growing/decaying modes (referred to as the nonpropagating double instabilities in the text). Introduction of baroclinic effects immediately destroys the nonpropagatory nature of these modes by turning them also into Holmboe modes (see Fig. 9) and to connect what were otherwise (in classical Holmboe theory) two separated bands (in wavenumber) of Holmboe modes. The propagation speeds of these transformed modes is proportional to the degree of baroclinicity of the system Δ.

(ii) In the limit where we have a globally constant shear profile in an infinite domain with a density discontinuity (Sec. III B), we find curiously that shear behaves to stabilize disturbances. Of course, if the density variation is Rayleigh-Taylor unstable (i.e., $\Delta<0$), there can be instability but only if the unstable stratification is severe enough [see the dispersion relation (40)].

(iii) In reference to the same problem of Sec. III B, the Boussinesq limit of that problem shows no influence of shear whatsoever in the resulting normal-mode wavespeeds [i.e., the Boussinesq limit (42)], although the resulting eigenfunctions will still reflect some signature of the shear.

(iv) The TG equation is not limited to the classic Kelvin-Helmholtz dispersion relation in the limit where the

layer thickness goes to zero, i.e., when $h \to 0$. Instead, it is limited to the Boussinesq-Kelvin-Helmholtz result. There are two differences of note that follow from this. The first is that all unstable modes described by the Kelvin-Helmholtz analysis, which are fully baroclinic, have nonzero propagation speeds irrespective of whether or not the modes are unstable $[Im(c) \neq 0]$ or stable $[Im(c)=0]$. This propagation speed is associated with the center-of-mass frame of the fluid. Since the Boussinesq approximation neglects density variations not associated with buoyancy, it cannot reflect the vertical variation of the perturbed horizontal momentum fluxes above and below the density interface as discussed above. Thus the BKH analysis predicts that unstable modes appear stationary to the laboratory observer. The second difference has to do with the growth rates associated with these unstable modes: the BKH analysis overpredicts the growth rates in proportion to the degree of baroclinicity. This overprediction, however, becomes pronounced only when its upper limit is approached, i.e., $\Delta \to 2$.

Experiments and observations

It is natural to inquire as to whether these baroclinic effects have any bearing on the results of experiments and observations made thus far. A recent laboratory study reported by Zhu and Lawrence considers Holmboe's instability as manifesting itself in the exchange flow of two different density fluids passing over each other in a constant-width channel.[7] An order-of-magnitude calculation using numbers typical to their experiments shows that according to (1), their laboratory studies are within the Boussinesq regime.[20] More specifically, given their typical Richardson numbers and shear layer thicknesses ($J \sim 1/2$ and $\delta = 1$ cm, see their Fig. 3), the typical reduced gravity ($g' = g\Delta \sim 1.5$ cm s^{-2}, see their Table I) and the typical wavespeeds associated with the observed unstable Holmboe modes ($c_r \sim 0.5$ cm s^{-1}, see their Fig. 11) show that the quantity $\delta U \sim 1.7$ cm s^{-1} and $\bar{U}_z \sim 1.7$ s^{-1}, giving for the RHS of (1) the measure $\delta U \bar{U}_z \sim 3$ cm s^{-2}, which is sufficiently less than $g \sim 10^3$ cm s^{-2}. Note that the choice of δU comes from the difference of the sheared velocities (i.e., $\delta U \sim |\bar{U}_+ - \bar{U}_-|$) and not from the wavespeed c_r since the latter is dominated by the former.

Observations reported by Oguz *et al.*[21] similarly suggest that the two-layer exchange flow taking place in the Bosphorus Strait is also within the realm of the Boussinesq approximation. The strait is characterized by fresh (less dense) water from the Black Sea flowing atop and opposite to salty (more dense) water flowing from the Sea of Marmara. That stretch of the strait where the flow is tightly constricted measures about 31 km, while the average depth is about 50 m (this does not include the sill that is located near the Marmara side of the strait). The transition layer between the salty and fresh water lies midway down in depth and has a typical transition zone thickness of 5 m [see their Fig. 3(c)]. The difference in velocities between the Marmara-ward flowing fresh water versus the Black Sea-ward flowing salty water is estimated at about 0.5 m s^{-1}, although this too depends on one's location with respect to the sill [see their Fig. 5(d)]. From the reduced gravity, they estimate from the data ($g' \sim 0.81$ m s^{-2}, see their Table I and the related salinity graphs) that one may liberally estimate $\Delta < 0.1$. A further liberal assumption would be to state that the shear transition layer scales here the same as the thickness of the density transition zone. With this assumption, one may estimate $\bar{U}_z \sim 0.2$ s^{-1} leading to the baroclinic measure $\delta U \bar{U}_z \sim 0.1$ m s^{-2}. We see here that despite these liberal estimates, the flow here does not feel with any significance the baroclinic effects considered here. Had we estimated the thickness of the shear layer by the depth of the Bosphorus Strait instead, the estimated measure of $\delta U \bar{U}_z$ would be ten times less.

These two examples show that at least as far as terrestrial oceanographic conditions are concerned, the Boussinesq approximation and the use of the TG equation are well-justified. A far more likely candidate in which the baroclinic effects discussed here may manifest is in the atmosphere. The mean wind at the atmospheric boundary layer, which is roughly at 1–2 km from the Earth's surface, is about 10 m s^{-1}, while at the base of the stratosphere (i.e., the tropopause, which marks the beginning of the temperature inversion), located at about 10–12 km, the mean flow is roughly 100 m s^{-1}.[22] These numbers give the estimate that $\delta U \bar{U}_z \sim 1$ m s^{-2}, which is only 10% of g. Although technically it means that this part of the atmosphere is also appropriately described by the BA and TG equations, it does suggest that baroclinic effects could manifest themselves and lend themselves to being observed in these physical conditions. It is possible that the baroclinic effects might be more pronounced on Mars. The extreme seasonal meridional winds observed on Mars are also 100 m s^{-1}, but because Mars' surface gravity is one-third of the Earth's, it would put the measure $\delta U \bar{U}_z$ on nearly equal footing with g there.

This work sets the stage toward developing a simple mechanistic description of the Holmboe instability, both within the Boussinesq and fully baroclinic treatments. Ongoing work to this end is aimed at applying and expanding the idea of the counterpropagating Rossby wave (CRW) "action at a distance" view to the physical scenario described in this work. As this viewpoint has been applied successfully to Rayleigh's problem,[13] here we are working toward including the interaction between the CRWs (which appear and propagate at the shear discontinuities) and those internal gravity waves appearing on the density discontinuities.

ACKNOWLEDGMENTS

The authors wish to thank one of the referees, who suggested we look deeper into the question of the Boussinesq approximation and its validity. Research supported by BSF Grant No. 0603414082, and by the Helen and Robert Asher Fund and the Technion Fund for the Promotion of Research. One of the authors is grateful to the ISF (Grant No. 0603414721).

APPENDIX A: PROCEDURAL REVIEW FOR PROBLEMS WITH DISCONTINUITIES

Problems involving discontinuities, such as a density jump in the classic Rayleigh-Taylor example or a step-like jump in the shear as in the classic Rayleigh problem, imply two fundamental conditions when one matches across the discontinuous dynamical surface, namely that (a) lest there be layer separation, there is a single interface and the normal velocities on either side of it must match, and (b) the stresses normal to the surface are also continuous. In nonviscous linearized problems such as the ones considered here (in which there is *no discontinuity in the steady velocity field* $\bar{U}$), the two conditions translate to (i) the vertical velocity being continuous across the interface, as well as (ii) the Lagrangian pressure perturbation. The manner in which these are instated is described below.

Inspection of the governing equations shows that when the background density field $\bar{\rho}$ and background shear $\bar{U}_z$ have step-like discontinuities, and when we restrict ourselves to two-dimensional motions, then the *normal-mode* response of the flow field away from these discontinuities is irrotational.[15,17] In other words, instead of solving for the stream function (see above), we may invoke the Cauchy-Riemann condition and represent the flow in terms of a potential ϕ, viz.,

$$\partial_x\phi = u = \partial_z\psi, \quad \partial_z\phi = v = -\partial_x\psi.$$

Given the normal mode ansatz, the potential must therefore satisfy Laplace's equation

$$(\partial_z^2 - k^2)\hat{\phi} = 0 \tag{A1}$$

everywhere away from the discontinuities. Furthermore, the Lagrangian equation of motion for an interface initially at rest at z, and subsequently perturbed, viz., $z \to z + \zeta_z(x,t)$, is given to linear accuracy by

$$ik[\bar{U}(z) - c]\hat{\zeta}_z = \hat{v}(z), \tag{A2}$$

where the position of the interface is denoted by $\zeta_z = \hat{\zeta}_z e^{ik(x-ct)}$ (the general equation of motion for an arbitrary interface initially at z is given by $\{\partial_t + [u(z') + \bar{U}(z')]\partial_x\}\zeta_z = v(z')$, in which z' is evaluated at the position of the moving boundary, $z + \zeta_z$).

If the vertically varying horizontal basic velocity field (i.e., $\bar{U}$) is continuous, then, to linearized accuracy, the vertical velocities above and below an interface, located at some position z, must be equal. The continuity of the vertical velocities means that the gradients of the velocity potentials must match from above and from below the interface (denoted by "$\pm$" subscripts, respectively), i.e.,

$$\partial_z\hat{\phi}_+ = \partial_z\hat{\phi}_-.$$

The meaning of our notation here is that for any quantity $f(z)$, we have that

$$f_\pm(z) \leftrightarrow \lim_{z' \to z^\pm} f(z'),$$

where $z^\pm$ indicates the approach to z from either above or below (respectively).

On the other hand, the total Lagrangian pressure of a fluid parcel, Π, can be written in terms of Eulerian variables as

$$\Pi(z, \zeta_z, t) = \bar{P}(z + \zeta_z) + P(z + \zeta_z, x, t). \tag{A3}$$

Because this is a linear theory and since all dynamical quantities are infinitesimal, expanding the above to first order reveals

$$\Pi(z, \zeta_z, t) = \bar{P}(z) - \bar{\rho} g \zeta_z + P(z, x, t) + \cdots. \tag{A4}$$

Continuity of this quantity across the dynamical surface means that $\Pi(z', \xi, t)|_{z' \to z^+} = \Pi(z', \xi, t)|_{z' \to z^-}$. In terms of the current problem and since $\bar{P}(z)$ is everywhere continuous, matching of the dynamical Lagrangian pressure across the moving surface means matching

$$-g\rho_+\hat{\zeta}_z + \hat{P}_+ = -g\rho_-\hat{\zeta}_z + \hat{P}_-, \tag{A5}$$

where $P_\pm = \hat{P}_\pm(z)e^{ik(x-ct)} + \text{c.c.}$ is the Eulerian pressure fluctuation above and below the moving boundary, respectively. We may explicitly express this piece of the total pressure by consulting (8) to obtain

$$-\frac{ik}{\rho_\pm}\hat{P}_\pm = ik(\bar{U} - c)u_\pm + \bar{U}_z v_\pm. \tag{A6}$$

APPENDIX B: NORMAL-MODE CALCULATION

Laplace's equation (A1) must be satisfied in four zones defined as

$$\underline{\text{Zone 1}} \leftrightarrow z > \frac{h}{2},$$

$$\underline{\text{Zone 2}} \leftrightarrow 0 < z < \frac{h}{2},$$

$$\underline{\text{Zone 3}} \leftrightarrow -\frac{h}{2} < z < 0,$$

$$\underline{\text{Zone 4}} \leftrightarrow z < -\frac{h}{2}.$$

The solutions to $\hat{\phi}_i$ are each

$$\begin{aligned}
\hat{\phi}_1 &= A_1 e^{-k(z-h/2)}, \\
\hat{\phi}_2 &= A_2 e^{-kz} + B_2 e^{kz}, \\
\hat{\phi}_3 &= A_3 e^{-kz} + B_3 e^{kz}, \\
\hat{\phi}_4 &= B_4 e^{k(z+h/2)}.
\end{aligned} \tag{B1}$$

The solutions are chosen so that all velocities exhibit decaying behavior as $z \to \pm\infty$. The relationships between all of the

coefficients A_i, B_i are determined by the matching conditions below. The velocity fields u_i and v_i in each corresponding Zone "i" are simply

$$\hat{u}_i = ik\hat{\phi}_i, \quad \hat{v}_i = \partial_z \hat{\phi}_i.$$

Because this particular problem has only one density interface, it will be enough to consider only its interface's equation of motion, which is, being at $z=0$,

$$ik(U_0 - c)\hat{\zeta}_0 = v(0). \tag{B2}$$

In order to proceed, we must match all the vertical velocities at each of the three corresponding interfaces, respectively, at $z=h/2$, $z=0$, and $z=-h/2$. These establish the first three relationships,

$$-A_1 = -A_2 e^{-kh/2} + B_2 e^{kh/2}, \tag{B3}$$

$$-A_2 + B_2 = -A_3 - B_3, \tag{B4}$$

$$B_4 = -A_3 e^{kh/2} + B_3 e^{-kh/2}. \tag{B5}$$

The continuity of the total Lagrangian pressure fluctuation across each of the three surfaces, according to the prescription in (A5), can be expressed with the aid of (A6) in each of the three instances. Since there is no density interface at $z=h/2$, the condition simplifies somewhat to

$$-k^2\left[\bar{U}\left(\frac{h}{2}\right) - c\right]A_1 - \Lambda_+ A_1 = -k^2\left[\bar{U}\left(\frac{h}{2}\right) - c\right](A_2 e^{-kh/2} + B_2 e^{kh/2}) - \Lambda A_1, \tag{B6}$$

where we have made use of (B3) in writing the last term on the RHS of (B6).

The stress condition at $z=0$ constitutes the most cumbersome of the resulting expressions,

$$-\frac{\bar{\rho}_+}{ik}[\Lambda k(-A_2 + B_2) + k^2 c(A_2 + B_2)] - \bar{\rho}_+ g\hat{\zeta}_0 = -\frac{\bar{\rho}_-}{ik}[\Lambda k(-A_2 + B_2) + k^2 c(A_3 + B_3)] - \bar{\rho}_- g\hat{\zeta}_0, \tag{B7}$$

where (B4) was used to rewrite the first term on the RHS of (B7). For convenience, we have introduced the notation $\bar{\rho}_\pm = \rho_0\left(1 \mp \frac{1}{2}\Delta\right)$. To supplement this, we explicitly write the equation for the interface,

$$-ikc\hat{\zeta}_0 = k(-A_2 + B_2), \tag{B8}$$

where we have again used (B4) in writing the RHS of (B8).

Lastly, since there is also no density interface at $z=-h/2$, the stress condition there becomes

$$-k^2\left[\bar{U}\left(-\frac{h}{2}\right) - c\right]B_4 + \Lambda_- B_1 = -k^2\left[\bar{U}\left(-\frac{h}{2}\right) - c\right](A_3 e^{kh/2} + B_3 e^{-kh/2}) + \Lambda B_4, \tag{B9}$$

where, in a similar fashion, we have made use of (B5) in writing the last term on the RHS of (B9).

The set (B3)–(B9) constitute seven equations for seven unknowns of the form

$$\mathbf{Mx} = 0,$$

in which $\mathbf{x} = (A_1, A_2, B_2, A_3, B_3, B_4, \hat{\zeta}_0)^{\mathbf{T}}$. Nontrivial solutions exist only if $\det(\mathbf{M}) = 0$. As a consequence, the following dispersion relationship must be satisfied for the complex wavespeed:

$$c^4 + a_1 c^3 + a_3 c^2 + a_3 c + a_4 = 0, \tag{B10}$$

where the individual coefficients appearing above are

$$a_1 = \frac{h}{4K}[e^{-K}\Delta(\Lambda_+ + \Lambda_- - 2\Lambda) + 2(\Delta\Lambda + \Lambda_- - \Lambda_+)], \tag{B11a}$$

$$a_2 = \frac{h^2}{8K^2}\{2e^{-2K}(\Lambda - \Lambda_-)(\Lambda - \Lambda_+) - e^{-K}(K+2)\Delta\Lambda(\Lambda_- - \Lambda_+) - 2\Lambda_-[\Lambda_+ + (K - 1 - \Delta)\Lambda] - 2\Lambda^2[1 + K(K + 2J - 2)] - 2\Lambda\Lambda_+(K + \Delta - 1)\}, \tag{B11b}$$

$$a_3 = -\frac{e^{-2K}h^3\Lambda}{8K^3}(\Delta\Lambda^2[1 + (K-1)e^K]^2 + (e^K - 1)\Lambda\Lambda_+ \times\{\Delta - e^K[2JK + \Delta(1-K)]\} + (e^K - 1)\Lambda\Lambda_- \times\{\Delta + e^K[2JK - \Delta(1-K)]\} + (e^K - 1)\Lambda_-\Lambda_+\Delta), \tag{B11c}$$

$$a_4 = \frac{e^{-2K}h^4 J\Lambda^2}{8K^3}\{\Lambda[1 + e^K(K-1)] + \Lambda_-(e^K - 1)\} \times\{\Lambda[1 + e^K(K-1)] + \Lambda_+(e^K - 1)\}. \tag{B11d}$$

The nondimensional terms J, K, and Δ are defined in the text. This calculation was verified using Mathematica 5.0.

[1] G. I. Taylor, "Effects of variation in density on the stability of superposed streams of fluid," Proc. R. Soc. London, Ser. A **132**, 499 (1931).
[2] S. Goldstein, "On the stability of superposed streams of fluids of different densities," Proc. R. Soc. London, Ser. A **132**, 524 (1931).
[3] J. Holmboe, "On the behavior of symmetric waves in stratified shear layers," Geofys. Publ. **24**, 67 (1962).
[4] Lord Rayleigh, "On the stability, or instability, of certain fluid motions," Proc. London Math. Soc. **9**, 57 (1880).
[5] L. N. Howard, "Neutral curves and stability boundaries in stratified shear flow," J. Fluid Mech. **16**, 333 (1963).
[6] L. N. Howard and S. A. Maslowe, "Stability of stratified shear flows," Boundary-Layer Meteorol. **4**, 5111 (1973).
[7] D. Z. Zhu and A. Lawrence, "Holmboe's instability in exchange flows," J. Fluid Mech. **429**, 391 (2001).
[8] S. P. Haigh and G. A. Lawrence, "Symmetric and non-symmetric Holmboe instabilities in an inviscid flow," Phys. Fluids **11**, 1459 (1999).
[9] S. P. Hazel, "Numerical studies of the stability of inviscid shear flows," J. Fluid Mech. **51**, 3261 (1972).
[10] W. D. Smyth and W. R. Peltier, "The transition between Kelvin-Helmholtz and Holmboe instability: An investigation of the over-reflection hypoth-

esis," J. Atmos. Sci. **46**, 3698 (1989).
[11]F. Lott, H. Kelder, and H. Teitelbaum, "A transition from Kelvin-Helmholtz instabilities to propagating wave instabilities," Phys. Fluids A **4**, 1991 (1992).
[12]A. Alexakis, "On Holmboe's instability for smooth shear and density profiles," Phys. Fluids **17**, 084103 (2005).
[13]E. Heifetz, C. H. Bishop, and P. Alpert, "Counter-propagating Rossby waves in the barotropic Rayleigh model of shear instability," Q. J. R. Meteorol. Soc. **125**, 2835 (1999).
[14]S. Chandrasekhar, *Hydrodynamic and Hydromagnetic Stability* (Clarendon, Oxford, 1961).
[15]P. G. Drazin and W. H. Reid, *Hydrodynamic Stability* (Cambridge University Press, Cambridge, UK, 1981).
[16]G. I. Taylor, *Scientific Papers* (Cambridge University Press, Cambridge, UK, 1971), Vol. IV.
[17]K. M. Case, "Stability of inviscid plane Couette flow," Phys. Fluids **3**, 143 (1960).
[18]G. A. Lawrence, F. K. Browand, and L. G. Redekopp, "The stability of a sheared density interface," Phys. Fluids A **3**, 2360 (1991).
[19]As an instance of the Howard-Miles' theorem.[15]
[20]It should be pointed out that their analysis demonstrated that the behavior predicted by the TG equation, as applied to their experimental setup, was verified by the observations, hence lending further support to the notion that the TG equation is an appropriate description of such systems.
[21]T. Oguz, E. Özsoy, M. A. Latif, H. İ. Sur, and Ü. Ülüata, "Modeling of hydraulically controlled exchange flow in the Bosphorus Strait," J. Phys. Oceanogr. **20**, 945 (1990).
[22]J. R. Holton, *An Introduction to Dynamical Meteorology* (Academic, New York, 1992).